Combination of Beamforming and Synchronization Methods for Epileptic Source Localization, using Simulated EEG Signals

Mahbubeh Azadehdel[1], Mohammad Reza Parsaei[1], Reza Boostani[1]

1. Biomedical Engineering Group, CSE & IT Dept, Faculty of Electrical and Computer Engineering, Shiraz University, Shiraz, Iran

Article info:
Received: 23 September 2011
First Revision: 14 October 2011
Accepted: 10 November 2011

Key Words:
EEG,
Localization,
Beamforming,
Synchronization,
Epilepsy.

A B S T R A C T

Localization of sources in patients with focal seizure has recently attracted many attentions. In the severe cases of focal seizure, there is a possibility of doing neurosurgery operation to remove the defected tissue. The prosperity of this heavy operation completely depends on the accuracy of source localization. To increase this accuracy, this paper presents a new weighted beamforming method to precisely localize the focal seizure sources from the electroencephalogram (EEG) signals. First, synchronization value is determined just between each two adjacent channels, and the channel with maximum average in synchronization index is selected as the nearest channel to the dominant focal sources. Next, weight of each channel is determined based on its Euclidean's distance to the selected channel. The determined weights act as a prior knowledge, incorporating in multiple signal classification (MUSIC) and some other beamforming methods to localize the exact place of seizure source. Next, the effect of estimated source is removed from the signals repeatedly to find the second focal source. This process continues till all focal sources being determined. To verify and validate the proposed scheme, 65 channels EEG signals were simulated and a linear weighting was applied to the three groups based on some sources. The proposed scheme and some known beamforming methods such as conventional beamformer, MUSIC, Weighted MUSIC, Capon's, Eigenvector and also SLORETA were applied to the simulated epileptic signals to find the location of sources. Experimental results reveal the superiority of the proposed method to the rival schemes in terms of localization accuracy, both in clean and noisy environments.

1. Introduction

Epilepsy is a recurrent seizure-related disorder of the central nervous system that affects approximately 1% of the world population (Khreisat, 2011). A seizure occurs when there is an increase in synchronous behavior of a localized group of pyramidal cells within the cerebral cortex, resulting in a surge of electrical activity. The over-stimulation at the seizure focus irritates neighboring regions, causing the seizure to spread. Some forms of epilepsy may be treated with medication while other types are medically intractable. For the latter, a suitable treatment option is to surgically remove the seizure focus. Therefore, a robust and accurate algorithm for localizing the seizure focus is necessary for successful surgical treatment (Russell & Koles, 2006).

**** Corresponding Author:***
Mahbubeh Azadehdel, PhD.
Biomedical Engineering Group, CSE & IT Dept., Faculty of Electrical and Computer Engineering, Shiraz University, Shiraz, Iran
Shiraz 71964-85115, Iran. Tel: +98-711-6473038. Fax:+98-711-6473575.
E-mail: azadehdel_3300@yahoo.com

Electroencephalogram (EEG) signals, which carry the physiological- basis information, are repeatedly used as a reliable source for this kind of diagnosis. A number of methods for localizing EEG sources have been investigated by different research teams (Latif et al., 2006). These methods totally can be divided into two categories: "equivalent current dipole" approach, in which the EEG signals are assumed to be generated by a relatively small number of focal sources, and the "linear distributed" approach, in which all possible source locations are considered simultaneously. However, the accuracy of such approaches is dependent on the number of both sources and sensors (channels). Moreover, mostly a head volume conductor and a source model need to be defined. Therefore, the associated computational complexity is generally very high (Latif et al., 2006).

The first approach to perform spatio-temporal data process, sampled at an array of sensors, was spatial filtering which has been mainly termed as beamforming in literatures. A beamformer is a mere application of Fourier-based spectral analysis to spatio-temporally sampled data. In other words, a beamformer performs spatial filtering to separate signals that have overlapping frequency content but originate from different locations (Van Veen & Buckley, 1988; Karim & Viberg, 1996).

A normal beamformer is a pure application of Fourier-analysis and source localization can be done by maximizing the output power. Due to the limitation of near-field beamformer on localizing sources with smaller bandwidth rather than far field ones (Zhi & Yan-Wah Chia, 2007); different weighting schemes have been developed to overcome these shortcomings. Furthermore, subspace-based methods have been deployed to extract the weights for recalculation of spatial spectrum.

On the other hand, synchronization of EEG signals between two by two channels can provide significant information from the brain cortical layer. In this study, due to the fact that most epilepsy sources expose in the brain cortical layer, utilizing synchronization values for reformulating the beamformer seems logical. In this way, phase synchronization index of the successive windowed signals are obtained as the significant information about the approximate location of the sources.

The remainder of this paper is structured as follows. In Section 2, used methods are briefly described. In Section 3, synchronization method and the proposed methodological strategy are introduced. In Section 4, data simulation and noise estimation are proposed. In Section 5, experimental results produced by applying the simulated data on the explained schemes are shown. Finally, Section 6 presents the conclusion, and opens a new horizon to future work.

2. Methods

In this section, the beamforming methods are expressed in a conceptual way rather than explaining its mathematical details. Suppose the head surface is molded by L electrodes, and EEG signals are recorded simultaneously. For an L-element electrode array of arbitrary geometry, the array output vector (EEG signal of all channels) is obtained as (Karim & Viberg, 1996; Huang et al., 2004; Ronhovde et al., 2002)

$$x(t,r,\theta)=a(r,\theta)s(t,r,\theta) \quad (1)$$

where s(t) is source vector, a(r,θ)contains coefficients that reflex attenuated source signal on the electrodes x(t,r,θ), and (r,θ) describe the location of each source or channel in the polar coordinate. The attenuation vector a(r,θ) depends on both angle and distance between the source and electrode. These coefficients construct the head model by which signals of channels can back project to the sources by multiplying the inverse of matrix a to the EEG signals arranged within the matrix x. As it is shown in Fig. 1, beamforming method acts as an inverse problem that estimates the position and signal of the source located at r0 from the origin.

In the presence of an additive noise n(t) we now get the model commonly used in array processing:

$$x(t,r,\theta)=A(r,\theta)\ \ s(t,r,\theta)+n(t) \quad (2)$$

where n(t) contains all disturbances and artifacts that undesirably are added to the EEG signals during the recording. The only consideration that should be taken is that the number of channels should be more than the number of sources. Therefore, this approach can just be applied to focal seizure that is faced with low number of seizure sources. However, it cannot be applied to EEG signals of patients with generalize seizure in which the whole brain acts like a distributed source. In this kind of seizure, the EEG signals contain infinite punctual sources.

The first attempt to automatically localize signal sources by means of electrode arrays was through beamforming techniques. The idea is to "steer" the array in one direction in a moment, and measure the output power. The steering location which results in maximum power produces the DOA estimates (Karim & Viberg, 1996).

In this study, the conventional beamformer was used. The conventional beamformer, mostly called Bartlett, is a natural extension of classical Fourier-based spectral analysis to sensor array of data. For an array of arbitrary geometry, this algorithm maximizes the power of beamforming output for a given input signal. Capon's beamformer, also known as the Minimum Variance Distorsionless Response filter in the acoustics literature, attempts to minimize the power contributed by noise and any signals coming from other undesired directions (Karim & Viberg, 1996).

In contrast to the beamforming techniques, the MUSIC algorithm provides statistically consistent estimates. Though the MUSIC method (Karim & Viberg, 1996) does not represent a spectral estimate, its important limitation is still failing to resolve closely spaced signals in small samples and at low SNR scenarios. This loss of resolution is more pronounced for highly correlated signals.

There has been attempts to improve/overcome some of MUSIC shortcomings in various specific scenarios. The most notable was the unifying theme of weighted MUSIC, which was particularized to various algorithms for different W. It is clear that a uniform weighting of the eigenvectors, i.e. W=I, results in the original MUSIC method. This is indeed the optimal weighting in terms of yielding estimates of minimal asymptotic variance. However, in difficult scenarios involving small sample, low SNR and highly correlated signals, a carefully chosen non-uniform weighting may still improve the resolution capability of the estimator without seriously increasing the variance (Karim & Viberg, 1996).

3. Synchronization

Synchronization, in general, means that many subsystems of a system respond in phase. In a brain subsystem, the term means that all neurons in that subsystem should fire at the same time. In the EEG literature, the term is used to denote that waves occur at the same time on both sides of the scalp. In other words, the phase of the two waves is the same (in-phase). For a single channel, the high amplitude, low frequency EEG denotes synchronization while the low amplitude, high frequency EEG denotes de-synchronization (Kushwaha & Malow, 1997).

Synchronization of different signals of EEG channels gives us considerable information about activity of cerebral cortex. Therefore, according to medical knowledge, since epilepsy sources are close to the cortex area, receiving synchronicity information in studies related to epilepsy is very important. There are several ways to check the synchronization between the signals; for example, the phase synchronization methods that can be defined based on FFT, Wavelet and etc. With regard to non-linear behavior of neurons, there are also ways to consider the chaos as the basis of phase synchronization.

In this study, phase synchronization is applied to improve the localization accuracy. Note that by assuming the stationary condition of EEG signals, we can use the FFT method for phase synchronization. For non-stationary signals, we must use the Wavelet method for phase synchronization.

3.1. Phase Synchronization

Definition: If α and β are two distinct phases, then they are synchronous if and only if $m\alpha - n\beta = C$, where C is a fixed number such that $0 \leq C < \pi$, where m and n are integers. For convenience of calculation, in this study, we shall keep $m = n = 1$ (Majumdar, 2009).

Let x_(j) (t) and x_k (t) be the EEG signals collected from the jth and kth electrodes, respectively. If x_(j) (t) and x_k (t) are synchrony signals, then the phase lag should be almost uniform across all harmonics. In this way, synchronization gives a measurement between x_(j) (t) and x_k (t) in a 0 (no synchronization) to 1 (perfect synchronization) scale (Majumdar, 2009).

Figs. 2 and 3 show two channels of synchronous EEG signals in time and phase domain. Although there is not complete likelihood in time domain between them in Fig. 2, Fig. 3 shows that when two signals have the same behavior, their phase is similar too.

3.2. Clustering

Here, clustering means the neighborhood construction for each EEG electrode. It should not be confused with clustering in pattern recognition. Neighborhood of a channel, here means the set of channels contain the desired channel and the channels closest to it. For example, for 60 channels, there are 60 neighborhoods or clusters. The i'th cluster has been formed according to the following rules:

1. Include the i'th Channel

2. Draw a circle centering the i'th channel so that at least one channel falls on the circumference and no channel is inside other than the i'th channel.

3. Include all the channels falling within the circumference.

In this study, the minimum Euclidean distance as the radius of a circle is used, and therefore, only one neighbor defines for every channel. Calculation of the average cumulative phase synchronization and the average cumulative signal power of the i'th cluster have been done according to the following equations:

$$P(i) = \frac{1}{|\Lambda|}\sum_{j\in\Lambda} syn(i,j) \quad (3)$$

$$W(i) = \frac{1}{|\Lambda|+1}\left(\sum_{j\in\Lambda} pow(j) + pow(i)\right) \quad (4)$$

Here, P(i) is the average cumulative phase synchronization in the i'th cluster, Λ is the set consisting of all the channels of the i'th cluster other than the i'th channel, |Λ| is the cardinality of Λ, W(i) is the average cumulative signal power of the i'th cluster, and pow(j) denotes the signal power at channel j. Since different clusters consist of different numbers of channels, we have taken the average of cumulative values of both the phase synchronization and power of each cluster in order to nullify the effects of channel population in a cluster (Majumdar, 2009).

3.3. Localization

After applying all the above steps on a EEG signal and finding the nearest electrode to a cortical source, by using a high threshold, we find the closest channel to the source with the knowledge that both the phase synchronization of a channel with its neighbors and the cumulative signal strength are high values near the cortical sources.

In the study, the high threshold value of 0.6 for the normalized signal and 0.2 for the phase synchronization was used, and if the signal was noiseless, the high threshold 0.4 for the phase synchronization was applied. After setting up the channels and holding (or satisfying) the above qualifications, in the next step, the number of repetitions of selected channels at various time intervals was considered. Channels that have all the above conditions will be introduced as the closest channels to the source. If this method is applied to the simulated signal with specified source, and the result of calculations by this method does not precisely define the same source, this is not a defect of this method. The source is located just under this electrode; but the direction of its bipolar is defined to the side of electrode, which is obtained from our simulation. So, values of power and phase synchronization of signal for this channel are higher than the others.

In the algorithm, shown in Fig. 4, a step-by-step procedure for source localization of this project is represented.

4. Data Simulation and Noise Estimation

Neural current sources in the brain produce external magnetic fields and scalp surface potentials that can be measured, using Magneto Encephalography (MEG) and EEG, respectively. The current fields in the head that produce these EEG and MEG (collectively E/MEG) signals can be separated into two components, the primary current term, representing the impressed neural and microscopic passive cellular currents, and the secondary or volume currents that are a result of the macroscopic electric field. In the context of the localization of neural sources, the forward problem is then to determine the potentials and magnetic fields that result from primary current sources. The inverse problem is to estimate the location of these primary current sources.

The emphasis in E/MEG modeling is, therefore, the relationship between a primary current source distribution and the data at the sensor array. The linearity of the forward model can be expressed as the inner product of a vector lead field and the primary current. To simplify the presentation here, the primary current to current dipoles are restricted, since more complicated sources can be expressed as sums or integrals of these elemental sources. Solutions are described to the forward problem for EEG by partitioning the lead field into the product of a sensor matrix, a kernel matrix, and the moment of the dipole. The most commonly used head model assumes that it is made up of a set of nested concentric spheres, each with homogeneous and isotropic conductivity. Under this assumption, the EEG problem admits to well-known closed form solutions. Here, the forward solutions are described for both problems for the spherical model using kernel matrices. The matrices are explicitly stated here in Cartesian coordinates (Mosher et al., 1999).

4.1. The Forward Problem

For the biological signals of interest in EEG, the time-derivatives of the associated electric and magnetic fields are sufficiently small that they can be ignored in Maxwell's equations. The typical head model assumes

that the head may be represented by three to five regions: scalp, skull, cerebrospinal fluid, gray matter, and white matter, and that the conductivity σ(r) is constant and isotropic within these regions. The gradient of the conductivity is therefore zero except at the surfaces between regions, which allows the volume integrals to be reworked into surface integrals. We assume our volume can be divided into M + 1 region with conductivities σ_i,i=1,… ,M+1 , which includes the non-conducting region outside the head.

The key modeling assumptions are that the fields are quasi-static and the shape of the homogeneous regions of the head are known and of known constant isotropic conductivity (Mosher et al., 1999).

4.2. EEG and Spherically Symmetric Conductor

The simplest case in EEG is a single spherical shell head model, i.e., the entire conducting volume is modeled as a sphere of constant conductivity σ. Here, the form of the solution, presented by Zhang in (Zhang, 1995), is used. The single spherical shell is too unrealistic as a model for the head due to the large difference between the conductivities of brain and skull. The typical multi-shell spherical model includes three layers for the brain, skull, and scalp; some also include a cerebrospinal fluid layer. The multi-shell case of spherical shells requires the evaluation of an infinite series.

When computing the solution to this forward problem, the infinite series must be truncated or approximated. Various approximations for the multi-shell case have been proposed. In this paper, the method proposed by Berg in (Berg & Scherg, 1994) is applied. For a given M-shell head model, these so-called “Berg parameters” can be designated as {λ_1,μ_1,λ_2,μ_2,λ_3,μ_3 }.

4.3. Matrix Kernel for Spherical Heads

If the primary sources were completely specified in location and moment, then implementation of the above formulas could proceed directly. The inverse problem, however, involves finding a suitable set of primary sources that adequately describe the data recorded by a limited set of sensors. As shown in Mosher et al. (1992), the inverse problem can often be better approached if the linear moment parameters q are separated from the nonlinear location parameters r_q.

In this section, as shown in Mosher et al. (1999), we can define the solution from the last section as the product of a "field kernel" and the dipole moment. Each model solution will be represented as the EEG scalar v(r)=k^T (r,r_q)q, where k(r,r_q) is a 3 × 1 vector kernel. These field kernels are then combined with the sensor characteristics to yield discrete matrices of lead field, which are clearly separated from the dipole moments.

According to the relations represented in Mosher et al.(1999), for a 3-shell model we can write:

(5)

$$k_3(r,r_q)=\lambda_1 k_1(r,\mu_1 R_q)+\lambda_2 k_2(r,\mu_2 R_q)+\lambda_3 k_3(r,\mu_3 r_q)$$

where $\{\lambda_1,\mu_1,\lambda_2,\mu_2,\lambda_3,\mu_3\}$ are the Berg parameters. In this step, by using the table 1 (Xu et al., 2004), and knowing the position of the source and the sensors, it is easy to calculate the kernel, and literately, the 3-shell model of EEG can be found.

4.4. Noise Estimation

Noise estimation is an important issue in all areas of signal processing. As we noted in last sections, in some beamforming methods, at first, it is necessary to estimate the noise. There are several ways to noise estimation. In this study, the soft thresholding method was used. A soft thresholding technique is applied in an attempt to improve the accuracy of signals with low signal-to-noise ratios (SNR). We will remove noise from the signal and estimate the noiseless signal.

For de-noising, using soft thresholding, in the first step, the signal is divided into different windows. Then, the signal of every window is projected to an orthonormal basis. In the other words, the FFT is taken from signal. Afterward, the coefficients are sorted in descending order, squared and summed to produce the variable ψ_m. J samples of a white Gaussian are then generated to estimate the expected value and variance of the variable ψ_m. As with many modeling situations, an increase in the integer value J improves the accuracy of the estimation at the cost of computing power and time. A graphical depiction of the de noising process is represented in Fig. 5.

5. Simulation Results and Discussions

5.1. Data Simulation

In the recent section, the EEG signal simulation method was described completely. On this basis, it is possible to say that having the location of electrodes to record the signal is the first step in production of an EEG signal.

For this purpose, first consider a model for the head. In the current study, the standard model of 10-10 (65 channels) was used. It should be noted that when the number of channels increases, the localization scheme acts better. Afterward, by using the Brain-Storm software, the location of electrodes was obtained. In table 2 the schematic of some electrode positioning is represented.

In the next step, three groups of signals were produced:

1. EEG signals with single-source localized at the frontal-temporal left or right side of the head.

2. EEG signals with punctual sources localized at the frontal-temporal of the head.

3. EEG signals with distributed sources within the head.

According to the clinical information of epilepsy, the focal epilepsy sources are in the frontal-temporal area and the cortical region of the brain. In the first group, by using the Fig. 6, the location of the source for different data is specified. 10 signals are found with the source placed on the right side and close to the electrodes Fp1, F7 and Af7, as shown on Fig. 6, and 10 other signals with the source placed on the opposite side and close to the electrodes Fp2, F8 and Af8 and at a depth of approximately 2.2 cm. For the second group, three closely sources were placed in the same area. The signals of the third group, are achieved by three sources located at different areas of the head and are almost simulated the global epilepsy.

For all of these three groups, source is a sinusoid with three different harmonics

(6) $s(t)=\sin(\pi t/2)+\sin(\pi t/4)+\sin(3\pi t/2)$

,

(7) $P(\sigma,\mu)\sim N(0,1)$

It is the source of noise near the epilepsy sources. The obtained signals were recorded by sampling rate 128 sam. /sec in about 2 minutes (i.e. 16000 samples). Also, it is necessary that 2 channels are assumed as the earth (reference), therefore there are only 63 channels.

In Figs. 7, 8 and 9, the samples of these signals for an arbitrary channel of noise-less data and in Fig. 10, a sample of a signal for an arbitrary channel of noisy data are shown.

5.2. Noise Estimation

As described in section 4.4 and the algorithm represented in Fig. 5, the noise of signals can be calculated and the noise from the original signals removed. Fig. 11 shows a primary, estimated noise-less and noise estimation of signal, for an arbitrary channel.

5.3. Beamforming Methods Implementation

In this section, the beamforming methods described in section 2 were used. At first, a Lead field matrix is necessary. The Brain-Storm software for calculation of this matrix was applied. The next step is working with maximization and minimization of the power function for the source localization. Although LORETA based methods are designed for correlated sources while beamforming methods are assumed based on independent sources, SLORETA is applied to simulated EEG signals and to compare its results with the other applied methods in this paper (Sekihara et al., 2005).

As studied, punctual sources are the same as a single source. The distributed sources are more irregular than the others, but in general, it is true to say that the WMUSIC methods have the minimum accuracy while the Conventional beamfromer (bf), in average, has the best accuracy.

5.4. Synchronization

To use the synchronization methods proposed in section 3, at first, it is necessary to define a neighborhood of electrodes. For every electrode, the Euclidean's distance to other electrodes is calculated, and the minimum of these distances will be found. It is obvious that, every electrode has only one neighbor. Afterward, by dividing the signal into time windows of 200 samples, the synchronization and power in every window of different channels are studied. By this method, the channel, neighbor with maximum value of synchronization, and power in every window can be obtained. Then, the channel in every window, which has the maximum value of synchronization and power, is selected as the closest

Table 1. Estimated Berg Parameters for 3-Shell Head Model

L	*Berg λl*	*Berg μl*
1	0.51346275	0.10663283
2	-0.45889827	0.098806681
3	0.062551069	0.32614976

NEUROSCIENCE

Table 2. The number and location of some electrodes

Number	Name	Type	Comment	Location	Weight
1	Fp1	EEG	AVERAGE REF	[0.10233; 0.03703; 0.02756]	[0.00000; 0.00000]
2	Fp2	EEG	AVERAGE REF	[0.10329; -0.03411; 0.02931]	[0.00000; 0.00000]
3	F4	EEG	AVERAGE REF	[0.06860; -0.05644; 0.09604]	[0.00000; 0.00000]
4	F3	EEG	AVERAGE REF	[0.06904; 0.06351; 0.08832]	[0.00000; 0.00000]
5	C3	EEG	AVERAGE REF	[0.01337; 0.07109; 0.11798]	[0.00000; 0.00000]
6	C4	EEG	AVERAGE REF	[0.00881; -0.06629; 0.12502]	[0.00000; 0.00000]
7	P4	EEG	AVERAGE REF	[-0.05785; -0.04645; 0.12011]	[0.00000; 0.00000]
8	P3	EEG	AVERAGE REF	[-0.05316; 0.05598; 0.11294]	[0.00000; 0.00000]
9	O2	EEG	AVERAGE REF	[-0.08635; -0.03571; 0.07554]	[0.00000; 0.00000]
10	O1	EEG	AVERAGE REF	[-0.08293; 0.03991; 0.07072]	[0.00000; 0.00000]
11	F8	EEG	AVERAGE REF	[0.03567; -0.07747; 0.04631]	[0.00000; 0.00000]
12	F7	EEG	AVERAGE REF	[0.04473; 0.07734; 0.04155]	[0.00000; 0.00000]
13	T8/T4	EEG	AVERAGE REF	[-0.01189; -0.08315; 0.05781]	[0.00000; 0.00000]
14	T7/T3	EEG	AVERAGE REF	[-0.00978; 0.08329; 0.04781]	[0.00000; 0.00000]
15	P8/T6	EEG	AVERAGE REF	[-0.05759; -0.06776; 0.06901]	[0.00000; 0.00000]
16	P7/T5	EEG	AVERAGE REF	[-0.05586; 0.06852; 0.06158]	[0.00000; 0.00000]
17	Pz	EEG	AVERAGE REF	[-0.05550; 0.00643; 0.13830]	[0.00000; 0.00000]
18	Fz	EEG	AVERAGE REF	[0.08864; 0.00106; 0.11618]	[0.00000; 0.00000]
19	IO1	EEG	AVERAGE REF	[0.07137; 0.04361; -0.03335]	[0.00000; 0.00000]
20	IO2	EEG	AVERAGE REF	[0.07281; -0.04416; -0.03404]	[0.00000; 0.00000]
21	AF9	EEG	AVERAGE REF	[0.05533; 0.06914; -0.00074]	[0.00000; 0.00000]
22	AF10	EEG	AVERAGE REF	[0.05293; -0.07036; 0.00536]	[0.00000; 0.00000]
23	F9	EEG	AVERAGE REF	[0.03067; 0.07735; 0.00751]	[0.00000; 0.00000]
24	F10	EEG	AVERAGE REF	[0.02609; -0.07823; 0.01914]	[0.00000; 0.00000]
25	CB1	EEG	AVERAGE REF	[-0.06755; 0.05743; 0.01767]	[0.00000; 0.00000]
26	CB2	EEG	AVERAGE REF	[-0.07926; -0.04810; 0.02327]	[0.00000; 0.00000]
27	TP7	EEG	AVERAGE REF	[-0.03196; 0.07948; 0.05498]	[0.00000; 0.00000]
28	TP9	EEG	AVERAGE REF	[-0.03746; 0.07484; 0.02512]	[0.00000; 0.00000]
29	TP10	EEG	AVERAGE REF	[-0.04789; -0.07197; 0.03208]	[0.00000; 0.00000]
30	TP8	EEG	AVERAGE REF	[-0.03302; -0.07820; 0.06251]	[0.00000; 0.00000]

NEUR SCIENCE

Table 3. Each channel column is repetition rate of synchrony one channel with its neighbor at all of windows. Data 1 is a signal with 3 distributed sources, data 2 is a signal whit single source and data 3 is a signal with 3 punctual sources.

Date	Channel 21	Channel 22	Channel 23	Mean of other Channel
1	82 %	77 %	86 %	15 %
2	85 %	12 %	25 %	16 %
3	14 %	91 %	15 %	12 %

NEUR SCIENCE

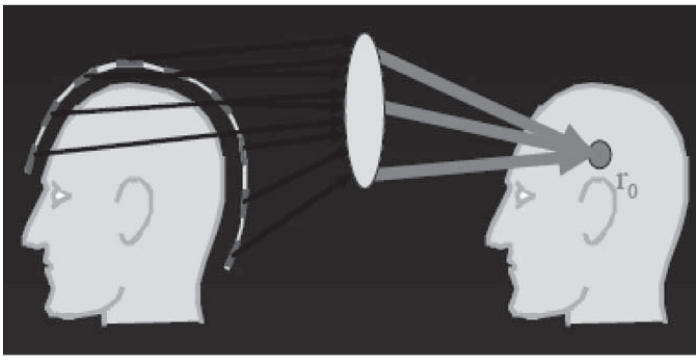

NEUROSCIENCE

Figure 1. The functionality of beamforming is simply depicted; the place and signal of source signal are estimated using back projection of all EEG channels.

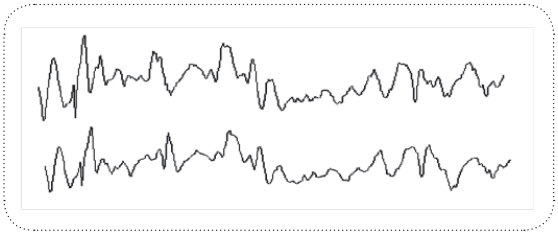

NEUROSCIENCE

Figure 2. Two channels of an EEG in time domain

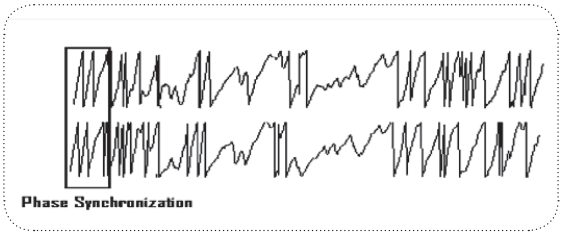

NEUROSCIENCE

Figure 3. Two channels of an EEG in Phase domain

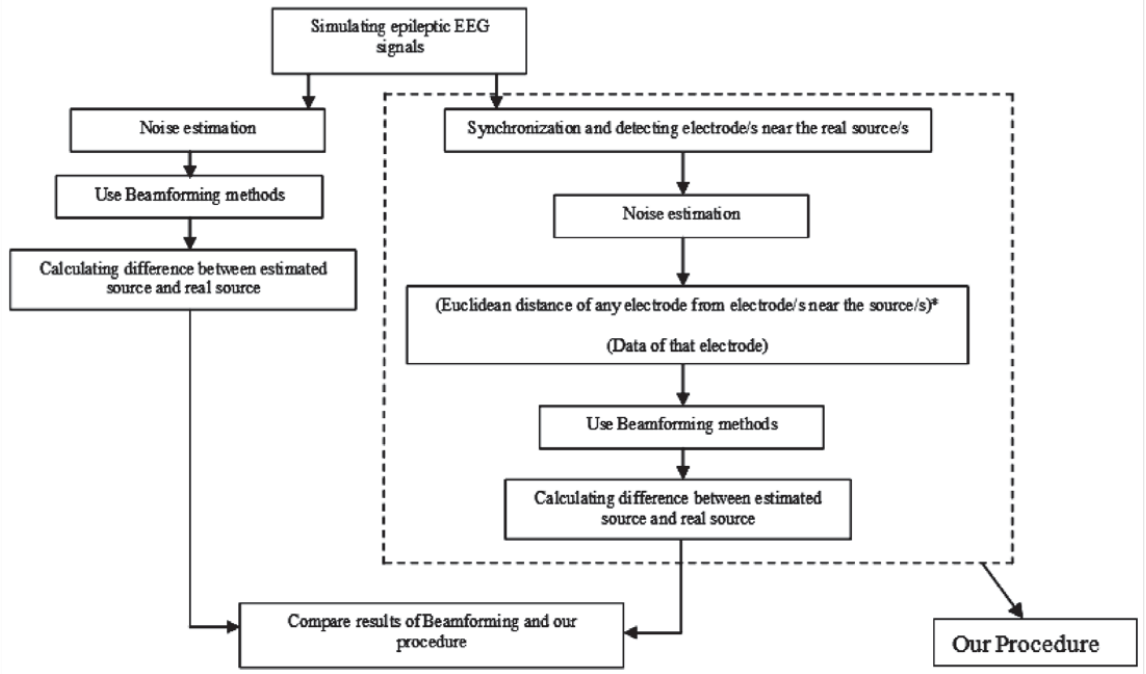

Figure 4. Step-by-step procedure for source localization

NEUROSCIENCE

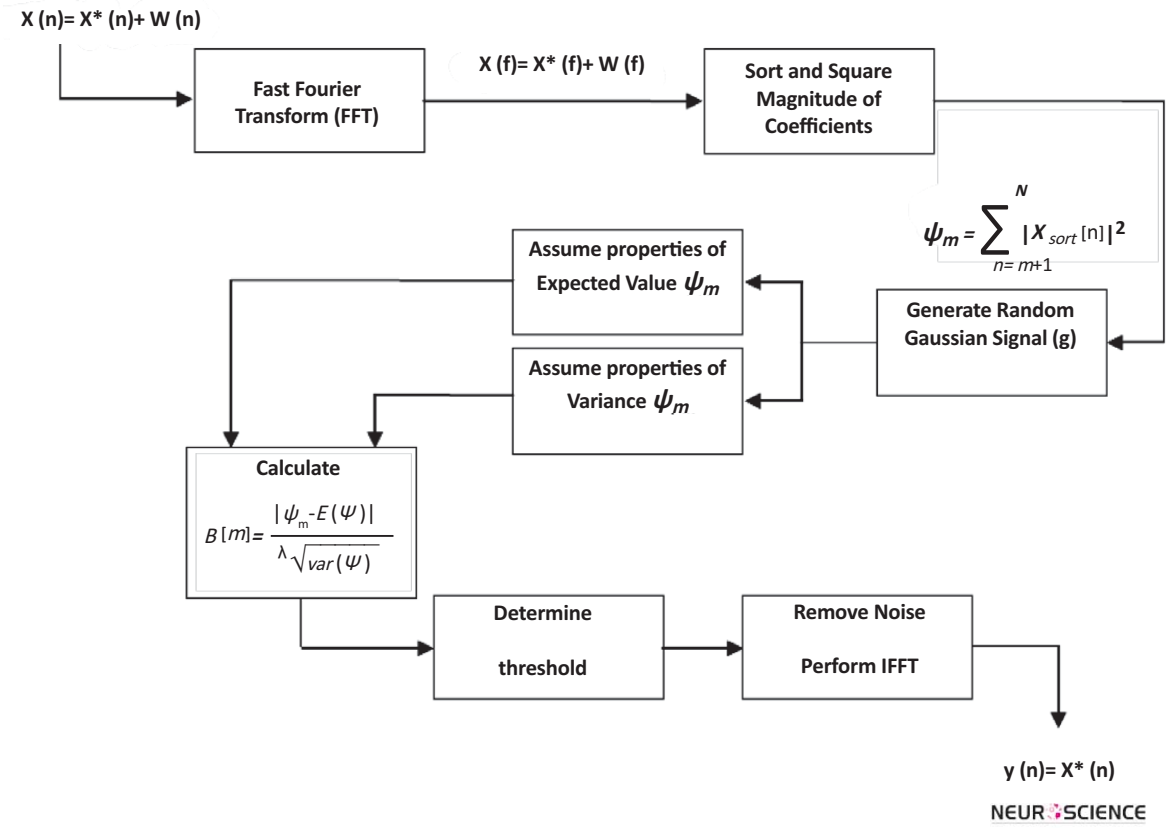

Figure 5. A graphical depiction of the denoising process, where x is the input signal, x* is the ideal, noiseless signal, w is the Gaussian noise, and the output, y is equal to the noiseless signal, x*.

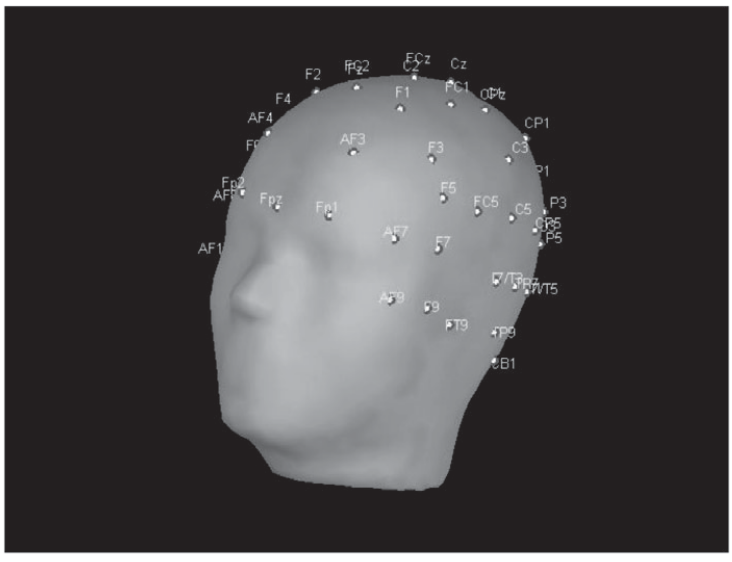

Figure 6. The schematic of electrode positioning

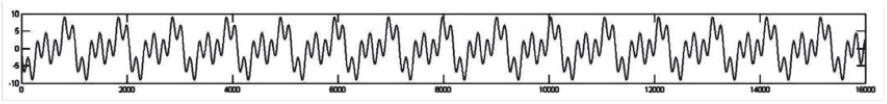

Figure 7. Simulated noise free signal of a single source

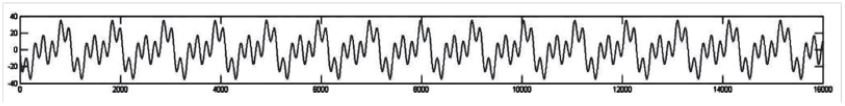

Figure 8. Simulated noise free signal of a distributed source

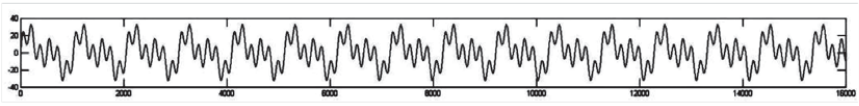

Figure 9. Simulated noise free signal of a punctual source

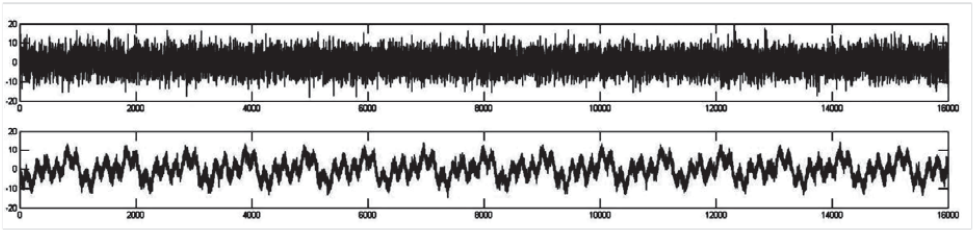

Figure 10. Simulated noisy signal of a single source

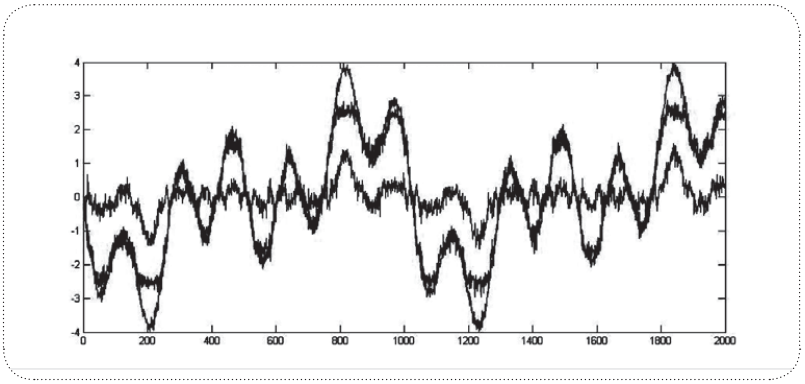

Figure 11. The blue signal is the primary, the black one is noiseless and the red one is the noise estimation.

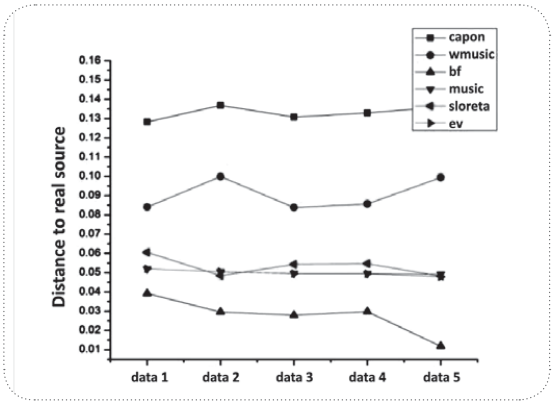

NEUROSCIENCE

Figure 12. The distance between real and localized source and a single source, before application of multiplication factor.

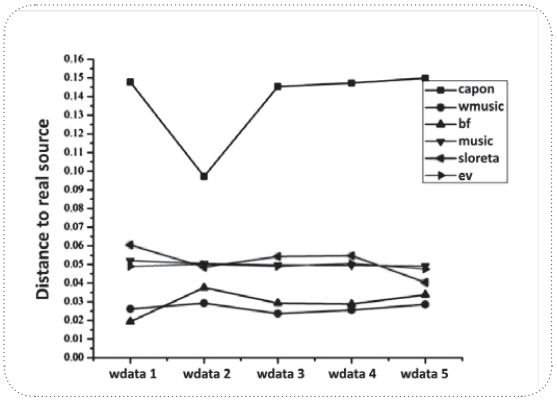

NEUROSCIENCE

Figure 13. The distance between the real and localized source and a single source, after application of multiplication factor.

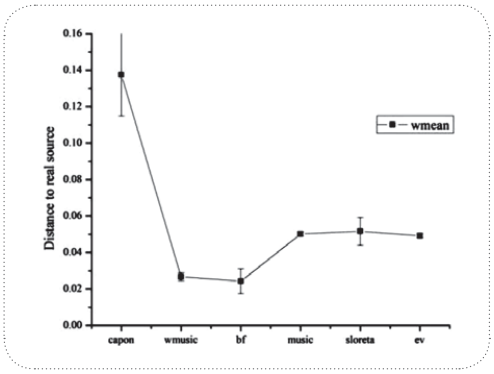

NEUROSCIENCE

Figure 14. The average and standard deviation of distance to the real source of a single source sample.

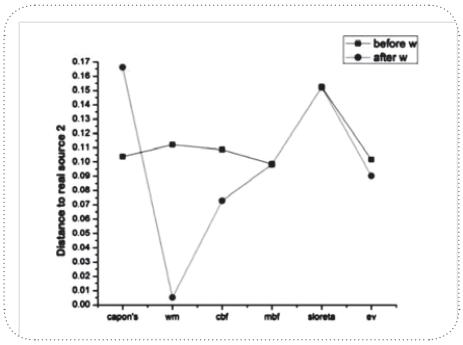

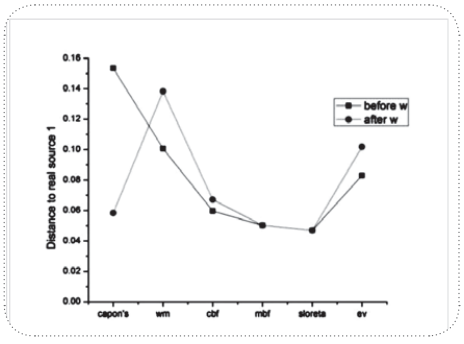

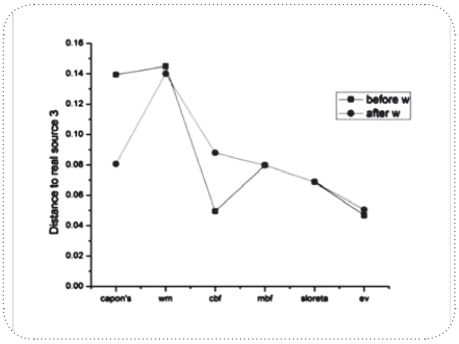

NEUROSCIENCE

Figure 15. The first stage of localization for signal with distributed sources.

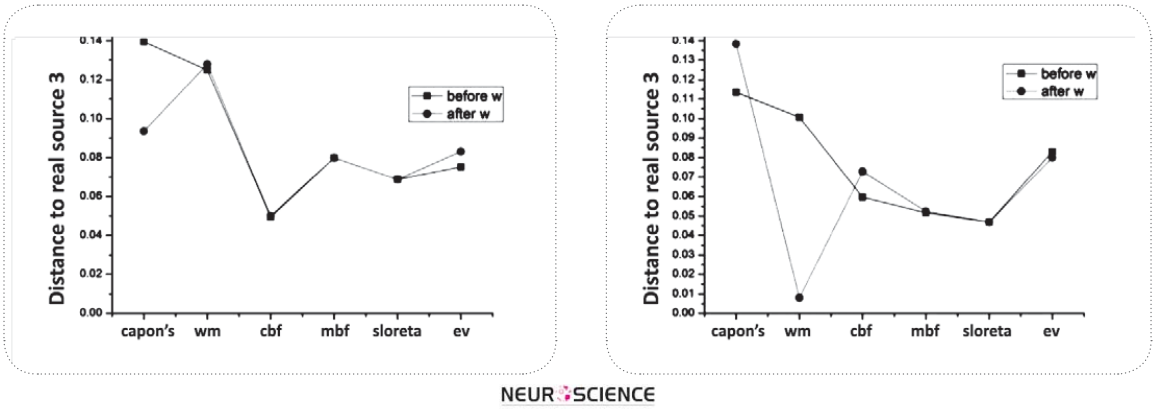

Figure 16. The second stage of localization for signal with distributed sources.

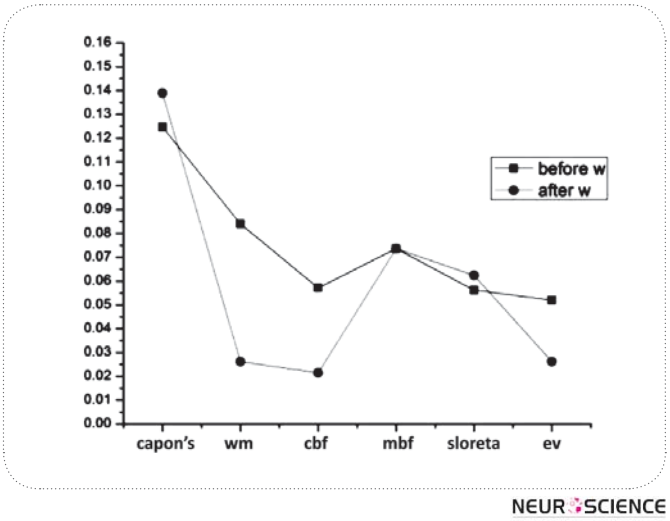

Figure 17. The third stage of localization for signal with distributed sources.

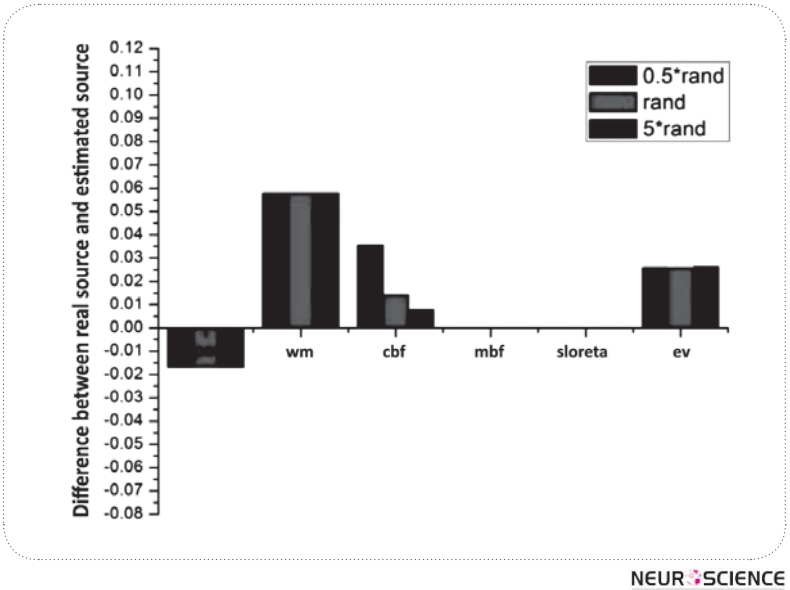

Figure 18. The noise effects and improvement multiplication for signal with a single source.

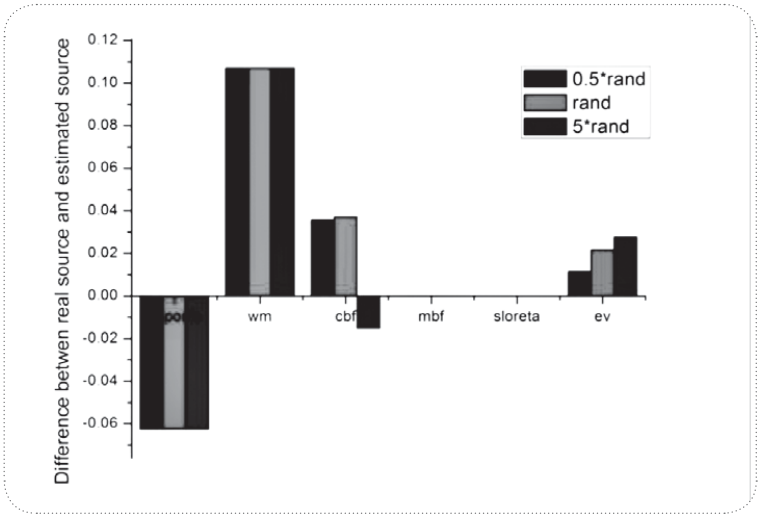

Figure 19. The noise effects and improvement multiplication for signal with distributed sources.

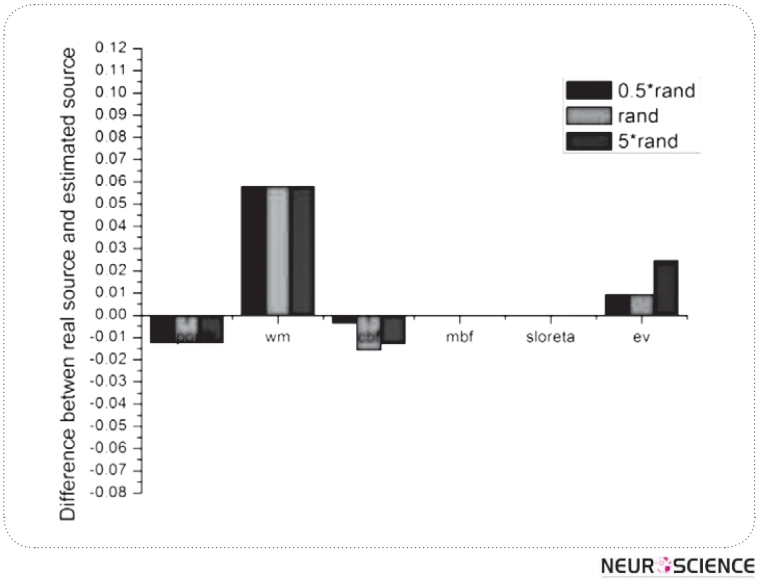

Figure 20. The noise effects and improvement multiplication for signal with punctual sources.

channel to the source. It is obvious that for signals with distributed sources, more than one channel is obtained. It is necessary to note that for specifying the maximum value of synchronization and power, it is crucial to define a threshold. In this study, high threshold power value of 0.6 was used for the normalized signal and 0.2 for the phase synchronization. Table 3 presents repetition rate of synchrony of one channel with its neighbor at all of the windows as an example to understand this section; This example is as to one channel in the different data with three types of sources.

5.5. Combination of Beamforming and Phase Synchronization Methods

Beamforming approach localizes the sources based on delay of the received signals of electrodes. In EEG processing, due to the small distance between sources and electrodes, this delay is very low; so that it's a disadvantage to apply beamforming for EEG localization. Using information of phase synchronization compensate this deficiency.

Now, the closest channel to the source has become clear. In this step, some data are changed, and this followed some changes in power functions of beamformers. It is assumed that the closest channel to the source is the "source channel". In cases of every synchronization method, it is possible to obtain only one channel, and to multiply data of every channel by the distance of obtained channel to the source channel. For the source channel, the 0.0000001 was used as the multiplication factor.

In this study, 3 channels near the sources are obtained for the signal of the distributed sources by using the synchronization method. In this case, the distances of every channel to the source channels are calculated and the minimum one is used as the multiplication factor. Also, for the source channels, 0.00000001 is used as the multiplication factor. It is obvious that for channels near the source, multiplication factors are smaller than channels away. So it is expected that beamforming methods, which have minimum noise of power as basis of localization, are better than before. Our criterion for evaluation of accuracy of results is the distance between real and estimated source.

From the results that obtained from a single source EEG signals, and by comparing Figs. 12 and13, it is clear that the distance from real source for WMUSIC to bf is decreased. For the methods as MUSIC, which is dependent on Eigen-vector of estimated noise, there is not much variation; because the multiplication factor of one matrix does not change corresponding Eigenvectors.

Fig. 14 shows the average and standard deviation of distance to the real source.

The results obtained from data analysis with punctual and distributed sources show that implementation of one stage beamforming of data localized only one source. Therefore, to find other sources, at first, the effects of this specified source are removed and then the resulted signal is given to the algorithm. This work is continued to find all sources.

In this study, to remove the effect of one source in one stage by nullifying the row corresponded to location of first channel in the following relation: (t)=w^H x(t), and then by multiplying w^(-H)in matrix, the data are returned to the primary signal space. In the resulted data, there is not any effect of specified source. Fig. 15 shows the first stage of the resulted data for the distributed sources.

As shown in Fig.15, one source is located as much as possible near to one of the real sources. In the next step, after removing the effect on this specified source, the next source was specified (Fig. 16) and then the last source is allocated (Fig. 17).

Above mentioned steps were repeated for localization of punctual sources. The results in general have the same diagrams, but the localized sources have less accuracy.

5.6. The Noise Effects

To study the noise effects on described methods, only for one data, the noise functions are implemented in three forms: randn, 5 × randn, and 0.5 × randn. Figs. 18, 19, and 20 show the noise effects on a single source signal. The first stage distributed sources signal and punctual sources signal, respectively. It is clear that improved multiplication factor is maximum for WMUSIC method.

6. Conclusion and Future Work

In this study, the source localization is presented for seizures with focal and global epilepsies, and by combination of two represented methods, it is tried to improve the results of localization. Main problems of localization methods are source localization accuracy and sensitivity of methods to noise. In the improved method, these problems are almost solved. Another advantage of this method is being non-invasive.

The results show that combination of two applied procedures for signals with single source has the best accuracy for conventional beamforming; but standard deviation for their results is much higher than WMUSIC. It can be said that WMUSIC method has more reliable results. Moreover, signals with punctual sources follow the same results. Results for signals with distributed sources show that WMUSIC has the best performance and minimum sensitivity to noise.

For future studies, it is suggested to apply Adaptive Beamforming methods to source localization. Also it is possible to combine EEG signals and MRI images. This procedure was applied on simulated EEG signals. Applying real EEG data validates our approach and its results.

References

Berg, P., & Scherg, M. (1994). A Fast Method for Forward Computation of Multiple-Shell Spherical Head Models.Electroenceph. Clin. Neurophysiol. , 90, 58-64.

Huang, M. X., Shih, J. J., Lee, R. R., Harrington, D. L., Thoma, R. J., Weisend, M. P., Hanlon, F., Paulson, K. M., Li, T., Martin, K., Miller, G. A., & Canive, J. M. (2004). Commonalities and Differences Among Vectorized Beamformers in Electromagnetic Source Imaging. Brain Topography, 16(3).

Karim, H., & Viberg, M. (1996). Two Decades Of Array Signal Processing Research. IEEE SIGNAL PROCESSING MAGEZINE.

Khreisat ,W. (2011). Clinical Applications of Electroencephalogram in Children. BCN, 2(3), 68-72.

Kushwaha, R. K., & Malow, B. A. (1997). A New Measure of EEG Synchronization.19th International Conference - IEEE/EMBS, Oct. 30 – Nov. 2, Chicago, IL. USA.

Latif , M. A., Sanei, S., Chambers, J., & Shoker, L. (2006). Localization of Abnormal EEG Sources Using Blind Source Separation Partially Constrained by the Locations of Known Sources. IEEE SIGNAL PROCESSING LETTERS, 13(3).

Majumdar , K. (2009). Constraining Minimum-Norm Inverse by Phase Synchronization and Signal Power of the Scalp EEG Channels. IEEE TRANSACTIONS ON BIOMEDICAL ENGINEERING, 56(4).

Mosher , J. C., Leahy, R. M., & Lewis, P. S. (1999). EEG and MEG: Forward Solutions for Inverse Methods. IEEE TRANSACTIONS ON BIOMEDICAL ENGINEERING, 46(3).

Mosher, J., Lewis, P., & Leahy, R. (1992). Multiple Dipole Modeling and Localization from Spatio-Temporal MEG data. IEEE Trans. Biomed. Eng. , 39, 541-557.

Ronhovde, R., Yang, L., Taxt, T., & Holm, S. (2002). High-Resolution Beamforming for Multibeam Echo Sounders Using Raw EM3000 Data. IEEE, 2, 923-930.

Russell , J. P. & Koles, Z. J. (2006). A Comparison of Adaptive and Non-Adaptive EEG Source Localization Algorithms Using a Realistic Head Model. Engineering in Medicine and Biology Society, 972-975.

Sakkalis, V., Giurcaneanu, C. D., Xanthopoulos, P., Zervakis, M. E., Tsiaras, V., Yang, Y., & Karakonstantaki, E. (2009). Assessment of Linear and Nonlinear Synchronization Measures for Analyzing EEG in a Mild Epileptic Paradigm. Ieee Transactions On Information Technology In Biomedicine, 13(4).

Sekihara, K., Sahani, M., Nagarajan, S. S., (2005). Localization bias and spatial resolution of adaptive and non-adaptive spatial filters for MEG source reconstruction. NeuroImage, 25, 1056– 1067.

Xu, X. L., Xu, B., & He, B. (2004). An Alternative Subspace Approach to EEG Dipole Source Localization. Phys. Med. Biol., 49, 327-343.

Zhang, Z. (1995). A Fast Method to Compute Surface Potentials Generated by Dipoles Within Multilayer Anisotropic Spheres. Phys. Med. Biol., 40, 335-349.

Zhi, W., & Yan-Wah Chia, M. (2007). Near-Field Source Localization via Symmetric Subarrays. IEEE SIGNAL PROCESSING LETTERS, 14(6).